Numerical investigation of internal ballistics in solid rocket motors using a multi-step simulation method

Duong Quoc Viet*, Nguyen Hanh Hoan, Phan The Son, Hoang The Dung

Institute of Missile, Academy of Military Science and Technology, 17 Hoang Sam, Nghia Do, Hanoi, Vietnam.

*Corresponding author: vietanh.140914@gmail.com

Received 05 Jun. 2026; Revised 20 Aug. 2026; Accepted 04 Sep. 2026; Published 16 Sep. 2026.

DOI: https://doi.org/10.54939/1859-1043.j.mst.FMC.2026.37-44

ABSTRACT

This paper presents a study on the internal ballistic calculation of a solid rocket motor using a multi-step simulation approach. The proposed method employs the CFX solver to simulate the thermodynamic behavior of combustion products within the combustion chamber and nozzle over time. The computational model is updated after each time step, accurately reflecting the evolution of the propellant grain geometry and the volumetric expansion of the combustion chamber during the burning process. The study was applied to a solid rocket motor with an inner diameter of 360 mm, utilizing a single-perforated cylindrical grain with partially milled slots. Experimental thrust measurements demonstrated a discrepancy of less than 2.5% compared with the simulation results, thereby validating the accuracy and reliability of the proposed model. This research provides a scientific basis for the development of advanced simulation tools to support the design and performance prediction of rocket motors under practical operating conditions. Furthermore, the proposed approach contributes to reducing experimental costs, which is particularly significant for large-scale rocket motors with high manufacturing expenses.

Keywords: Solid rocket motor; Internal ballistics; Multi-step simulation; Composite propellant; Complex burning surface.

1. INTRODUCTION

Solid rocket motors (SRMs) are increasingly being employed in a wide range of applications, not only in military systems but also in aerospace and space missions. The development of propulsion systems with large payload capacities and requirements for high and stable thrust presents significant challenges for the domestic solid rocket motor industry. Alongside research efforts aimed at developing new propellant formulations with higher burning rates and greater energy output, considerable attention has also been devoted to the design of propellant grain geometries. Special burning configurations, such as star-shaped perforations, cruciform perforations, and grains incorporating additional slots or grooves, have been widely adopted to achieve higher thrust levels and tailor the thrust-time profile of rocket motors [1-3].

One of the major challenges in propellant grain design is controlling the variation of the burning surface area throughout the combustion process [2, 4]. For propellant grains with complex geometries, such as asymmetric configurations or shapes that are not axisymmetric, deriving analytical expressions for the evolution of the burning surface area is often impractical. Consequently, the investigation of internal ballistics and motor operating characteristics using conventional analytical methods becomes highly challenging [3-5].

Nowadays, numerical simulation tools have increasingly demonstrated their effectiveness and reliability in engineering analysis, significantly reducing the need for costly experimental testing. Three-dimensional simulations enable accurate determination of the propellant grain burning surface area at different stages of combustion, while also providing a realistic representation of the thermodynamic phenomena associated with the expansion of combustion products within the combustion chamber. As a result, the investigation of internal ballistic processes can be conducted with greater accuracy and closer agreement with experimental observations [6-8].

In this study, a multi-step simulation method supported by ANSYS CFX is employed to investigate the internal ballistics of a solid rocket motor. To achieve this objective, the computational domain is defined as the free volume inside the motor combustion chamber and nozzle, while the working fluid is modeled as a mixture of propellant combustion products. The thermodynamic behavior of the combustion gases is simulated using ANSYS CFX, whereas the evolution of the propellant grain burning surface is updated at each time step throughout the combustion process [4, 9, 10].

The multi-step simulation approach enables accurate determination of the propellant grain burning surface area throughout the combustion process, a task that is difficult or even impossible to accomplish using conventional analytical methods when dealing with complex grain geometries. Furthermore, three-dimensional simulations provide valuable insight into physical phenomena that influence motor performance, such as erosive burning and energy losses. These capabilities offer a reliable basis for optimizing both propellant grain and motor designs, thereby significantly reducing the cost and extent of experimental testing [9, 11].

2. COMPUTATIONAL METHODOLOGY

2.1. Simulation model development

2.1.1. Development of the three-dimensional model

To investigate the internal ballistics of the solid rocket motor, a computational domain was established as shown in Figure 1. The domain consists of the entire free volume enclosed by the motor casing and the propellant grain. The boundary conditions are defined as follows:

+ Inlet: All burning surfaces of the propellant grain (The geometry and dimensions of the propellant grain are presented in Figure 3 and Table 1);

+ Outlet: The nozzle exit cross-section.;

+ Wall: The inner surfaces of the motor casing and nozzle, as well as the inhibited surfaces of the propellant grain that are protected from combustion.

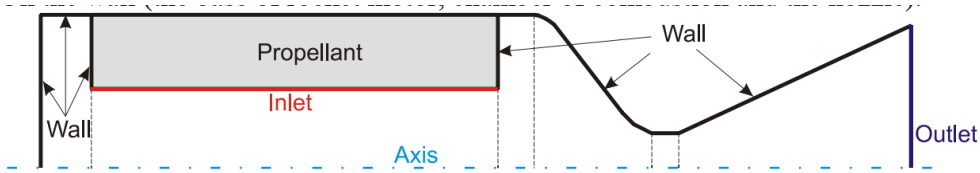


Figure 1. *Computational domain model.*

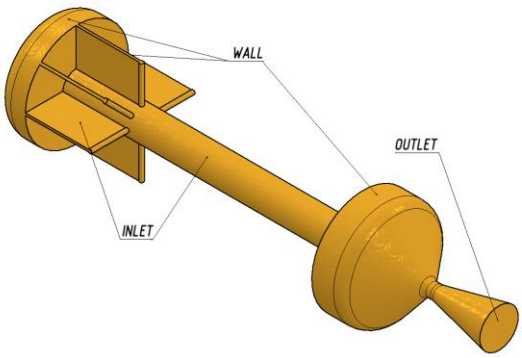


Figure 2. *3D Simulation model.*

A three-dimensional model of the computational domain was created using Autodesk Inventor (Figure 2) and subsequently imported into ANSYS CFX via the Geometry module for further numerical analysis.[6, 10].

Table 1. *Geometrical parameters of the propellant grain.*

No.	Parameter	Unit	Value
1	Length	mm	1000
2	Outer Diameter	mm	360
3	Inner Perforation Diameter	mm	100
4	Number of Slots	-	6
5	Slot Width	mm	10
6	Slot Depth	mm	200

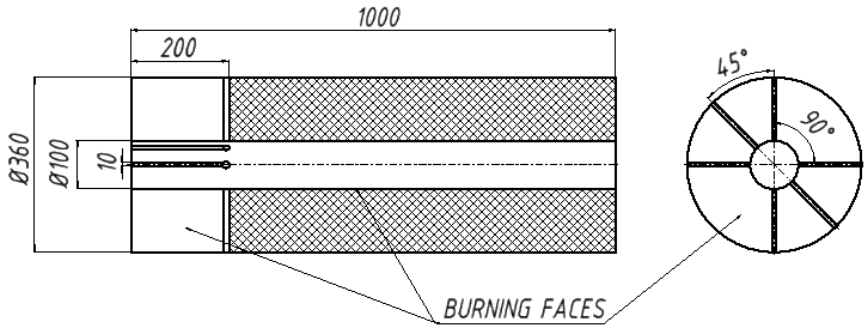


Figure 3. *Initial Propellant Grain Geometry.*

2.1.2. Mesh generation and computational domain discretization:

The mesh generation process was performed in the Mesh module using the CFX Solver Preference setting.[6]. An unstructured tetrahedral mesh was employed for the computational domain, complemented by prism layers near the wall boundaries to accurately resolve the near-wall flow characteristics. The final computational mesh consisted of 1,265,318 elements. Figure 4 illustrates the generated mesh on the symmetry plane of the computational domain.

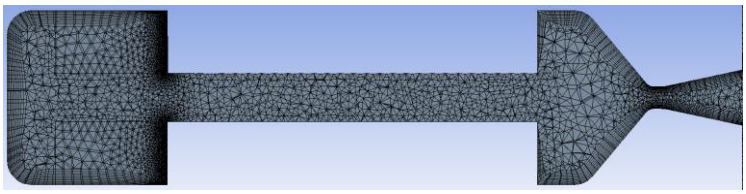


Figure 4. *Computational Mesh on the Symmetry Plane.*

2.1.3. Computational model

Using ANSYS CFX-Pre, the following flow and heat transfer models were selected for the numerical simulations [1]:

+ Turbulence model: The shear stress transport (SST) k–ω turbulence model was employed, as it is well suited for simulating supersonic flows within the nozzle and in the downstream exhaust region.

+ Heat transfer model: The total energy formulation was selected to solve the total energy equation of the combustion products, thereby accounting for the thermodynamic behavior of the flow.

2.2. Boundary conditions and convergence criteria

2.2.1. The following assumptions were adopted in the numerical model

- The propellant grain burns according to the geometric burning law, and the burning rate follows a power-law burning-rate equation;

- The specific heat ratio (k) and gas constant (R) of the combustion products are assumed to remain constant throughout the combustion process;

- The ignition transient phase is neglected.

2.2.2. Boundary conditions

- Inlet: A subsonic inflow boundary condition was specified. The mass flow rate of the combustion products entering the computational domain was determined by:

$$m = S \cdot u \cdot \rho$$

Where: m – Mass flow rate of the combustion products entering the computational domain, [kg/s];

S – Total burning surface area of the propellant grain (total inlet area), [m^2];

u – Propellant burning rate, [m/s];

ρ – Propellant density, [kg/m^3]

- Outlet: A supersonic outlet boundary condition was applied at the nozzle exit.

- Wall: All wall boundaries were defined as no-slip walls.

* The convergence criteria for the numerical simulations were specified as follows: Max interations: 200; Residual type: RMS; Residual target: 1e-6.

2.3. Multi-step simulation procedure

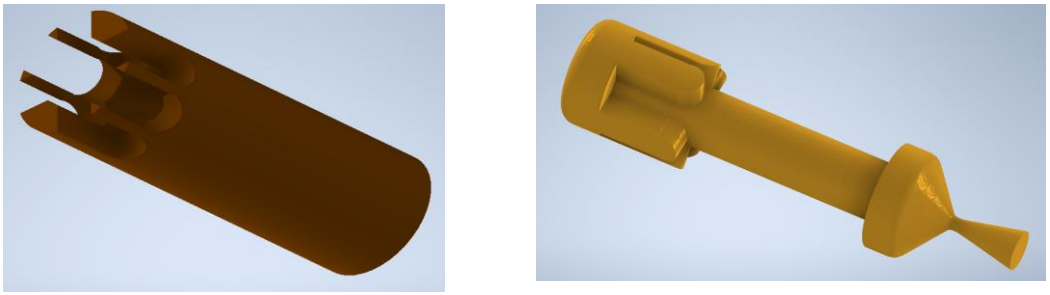
Step 1: The thermodynamic behavior of the combustion products within the combustion chamber and nozzle is simulated. The average chamber pressure and the thrust generated at the nozzle exit are recorded for each time step.

Step 2: The simulation model is reconstructed after each time increment Δt.

During the time interval Δt, the propellant grain regresses by a thickness Δe = u. Δt

Where: $u=u_1.p^v$ is the propellant burning rate, u_1 is the burning-rate coefficient, v is the pressure exponent of the burning-rate law, p is the combustion chamber pressure.

At time t_0+ Δt, all burning surfaces of the propellant grain are displaced along their local normal directions by a distance Δe. This procedure updates the grain geometry and the corresponding computational domain to account for propellant consumption during combustion. Figure 5 illustrates the propellant grain geometry and the computational domain at = 6.8 s (corresponding to a regression depth of Δe = 50 mm).



a *b*

Figure 5. *Propellant grain geometry and computational domain at t = 6.8 s*
a – Propellant grain; b – Computational domain.

Step 3: The computational model is updated, and the simulation is carried out to obtain the corresponding results.

2.4. Experimental thrust measurement

To validate the accuracy of the numerical simulation, a static firing test was conducted, during which the rocket motor was mounted on a test stand and its thrust was measured. The experimental thrust data were then compared with the simulation results to assess and validate the accuracy of

the proposed computational model.

3. SIMULATION AND EXPERIMENTAL RESULTS

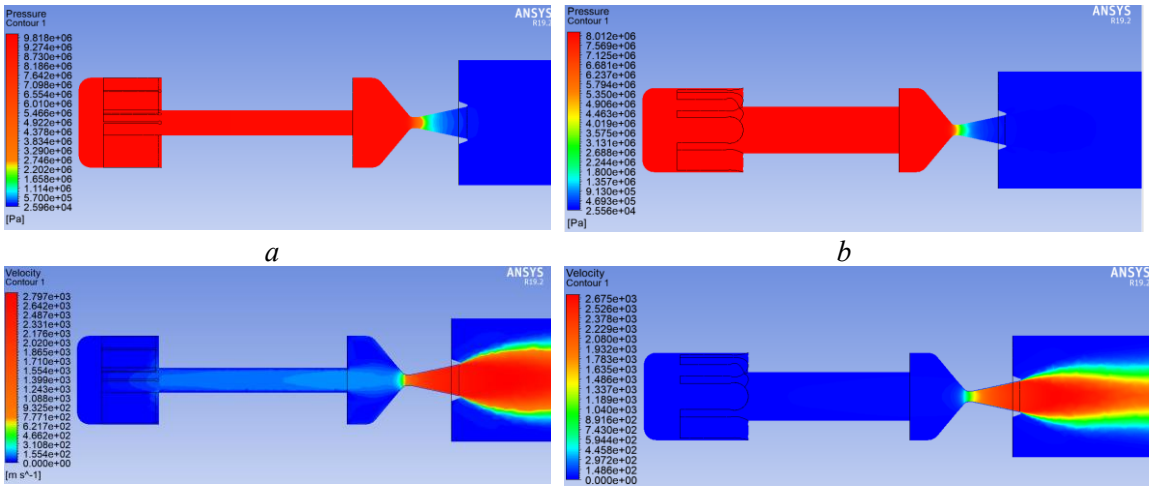
Experiments were carried out using a rocket motor and propellant whose specifications are presented in Table 2.

Table 2. *Parameters of the experimental propellant and rocket motor.*

No.	Parameter	Unit	Value
1	Propellant density	kg/m^3	1760
2	Burning-rate coefficient	-	29.77x10^{-5}
3	Pressure exponent of the burning-rate law	-	0.201
4	Motor inner diameter	mm	360
5	Nozzle throat diameter	mm	45
6	Nozzle exit diameter	mm	100

3.1. Simulation results

The results of the thermodynamic simulation of the combustion products inside the rocket motor are shown in Figure 6.



a *b*

c *d*

Figure 6. *Pressure and Velocity Distributions of the Gas Flow.*
a – Pressure distribution at t = 0.1 s; b - Pressure distribution at t = 6.8 s;
c – Velocity distribution at t = 0.1 s; d – Velocity distribution at t = 6.8 s.

The thrust of the rocket motor is determined using the following equation:

$$F = m \cdot v + p \cdot S_{cr}$$

Where: m – Mass flow rate at the nozzle exit, [kg/s];

v – Gas velocity at the nozzle exit, [m/s];

p – Pressure at the nozzle exit, [Pa];

S_{cr} – Cross-sectional area of the nozzle exit, [m^2].

The calculated thrust values of the rocket motor are presented in Table 3

Table 3. *Calculated thrust of the rocket motor.*

	1	2	3	4	5	6	7	8	9	10
t [s]	0.1	0.2	0.3	0.5	1	1.5	2	2.5	3	3.5
F [N]	25589	24793	24726	24640	24521	23730	23241	22869	22535	22215

	11	**12**	**13**	**14**	**15**	**16**	**17**	**18**	**19**	**20**
t [s]	4	4.5	5	5.5	6	6.5	7	7.5	8	8.5
F [N]	21956	21632	21222	20799	20420	20058	19659	19223	18885	18803
	21	**22**	**23**	**24**	**25**	**26**	**27**	**10**	**11**	**12**
t [s]	9	9.5	10	10.5	11	11.5	12	12.5	13	13.5
F [N]	18994	19282	19611	19920	20077	19962	19642	19297	19073	18922
	13	**14**	**15**	**16**	**17**	**18**	**19**	**20**	**21**	**22**
t [s]	14	14.5	15	15.5	16	16.5	17	17.5	18	18.2
F [N]	18724	18322	18158	18537	18854	19321	20166	12438	2389	0

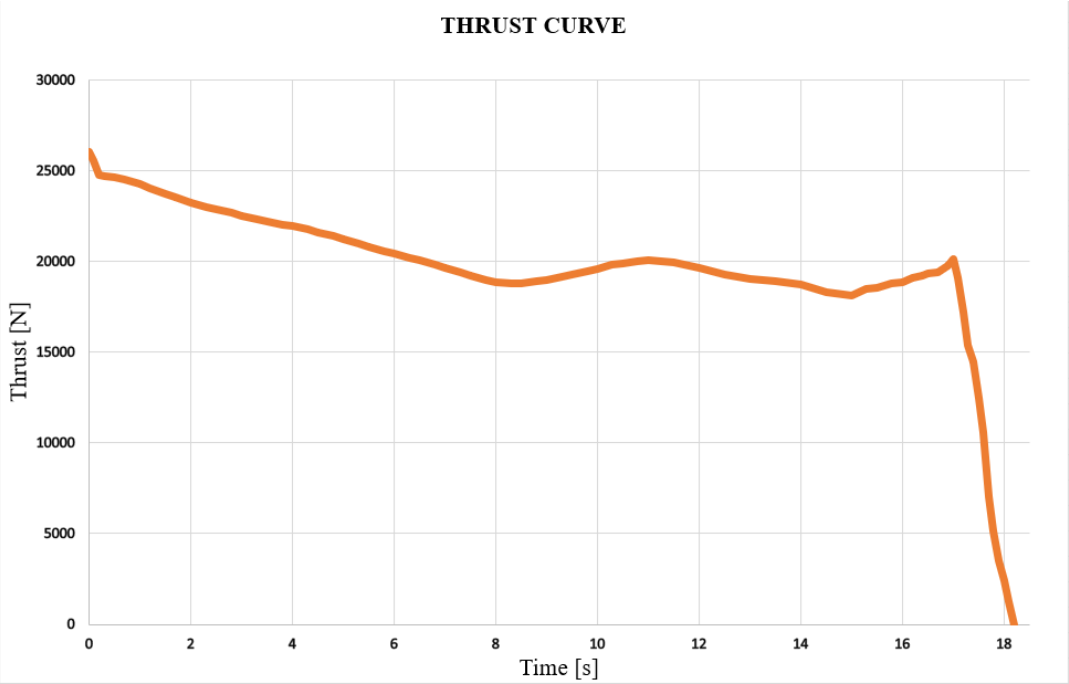


Figure 7. *Thrust-time curve.*

The simulation results show that the pressure is uniformly distributed within the motor combustion chamber, with a maximum pressure of 9.8 MPa at t = 0.1 s.

At the initial stage, when the inner perforation of the propellant grain is still small, a noticeable increase in the velocity of the combustion products is observed within the combustion chamber, with the flow velocity increasing toward the nozzle. However, at t = 6.8 s (when the diameter of the inner perforation reaches 200 mm), the gas velocity within the combustion chamber becomes negligible.

The calculated thrust results indicate that the motor operates for 18.2 s. The maximum thrust reaches 25589 N, while the average thrust is 20007 N.

3.2. Experimental results

The rocket motor with the specifications and configuration presented in Table 2 was tested on a dedicated test stand under ambient temperature conditions, and the thrust was measured. The measured results are shown in Figure 8.

The experimental results show that the maximum thrust of the rocket motor is approximately 28000 N. The high initial thrust is attributed to the additional energy supplied during the ignition process, at t = 0.1 s, the motor thrust is approximately 26000 N. The measured average thrust is 19545 N. Comparison with the calculated results shows a deviation of less than 2.5%.

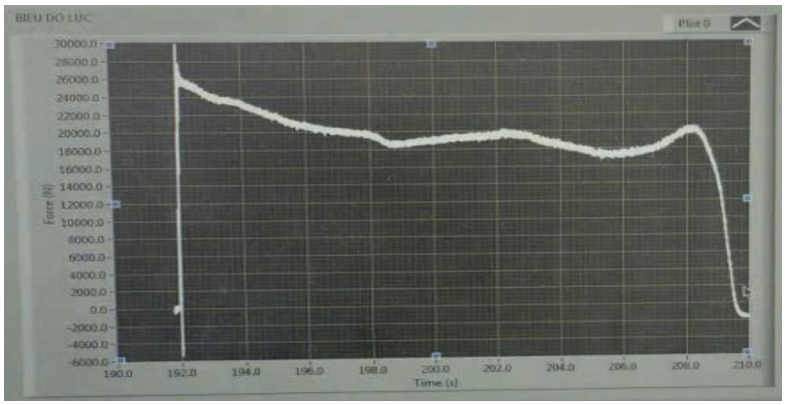


Figure 8. *Experimental rocket motor thrust results.*

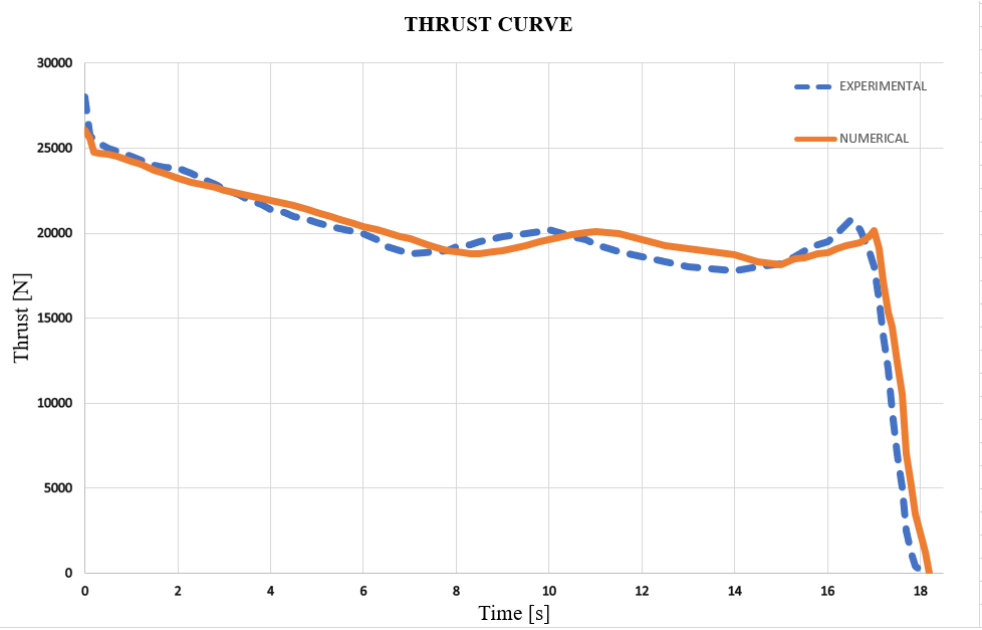


Figure 9. *Comparison of simulated and experimental rocket motor thrust.*

The simulation and experimental results show that the multi-step simulation method is capable of accurately calculating the internal ballistics of solid rocket motors. In addition, it has the capability to predict physical phenomena that affect motor performance. The small discrepancy between the experimental and simulation results confirms the effectiveness and reliability of the model for internal ballistics calculations.

4. CONCLUSIONS

This paper applied a multi-step simulation method to calculate the internal ballistics of a solid rocket motor. The method enables accurate prediction of the operating pressure and thrust of the motor, while also providing the capability to investigate and analyze physical phenomena that affect motor performance. This approach offers advantages over conventional analytical and numerical methods, in which many physical phenomena are neglected and the calculated parameters are assumed to be uniform throughout the combustion chamber.

The simulation and experimental results demonstrated that the multi-step simulation method can be applied to the design of solid rocket motors, particularly those employing propellant grains with complex burning surface geometries. This contributes significantly to reducing experimental

testing costs, especially for large-scale motors with high manufacturing costs.

Due to the limited scope of this paper, many aspects of the authors' research could not be presented in detail. Future work will focus on further developing the multi-step simulation method for motor performance prediction, taking into account the effects of phenomena such as erosive burning, erosion, and incomplete propellant combustion. These efforts will contribute to the development of an advanced simulation tool capable of supporting the design and prediction of rocket motor performance under realistic operating conditions.

REFERENCES

[1]. Phạm Thế Phiệt, *"Lý thuyết động cơ tên lửa"*, Học Viện Kỹ thuật Quân sự, Hà Nội, (1995) (in Vietnamese).
[2]. Lê Song Tùng và các tác giả, *"Tính toán thiết kế động cơ tên lửa nhiên liệu rắn"*, NXB Quân đội nhân dân, (2013) (in Vietnamese).
[3]. M.D. Phuong, B.D. Tan, D.Q. Viet. 2025. *"A study on developing a computational model for determining operating parameters of a dual-flow solid rocket engine"*. Journal of Military Science and Technology, vol 101: 140-147, https://doi.org/10.54939/1859-1043.j.mst.101.2025.140-147
[4]. Astakhova, T. P., & Tolkacheva, I. O., *"Ballistic Design of Flight Vehicles"*, Moscow State Technical University Press (MSTU), (1990).
[5]. Saulius RAČKAUSKAS, *"Numerical study on internal ballistics characteristics of a solid propellant rocket motor"*, MECHANIKA, vol. 25(3), pp. 187-196, (2019). DOI: 10.5755/j01.mech.25.3.23742
[6]. Ki, W.; Ko, T.; Kim, S.; Yoon, W., *"3D grain burnback analysis using the partial interface tracking method"*, Aerospace Science and Technology, vol. 68, pp. 58-67, (2017). DOI: 10.1016/j.ast.2017.04.023
[7]. Joel H. Ferziger, Milovan Peric, *"Computational Methods for Fluid Dynamics"*, Springer, (2020).
[8]. Pralits J.; Natali D.; Guerrero J.; Bottaro A., *"Wolf dynamics - multiphysics simulations, optimization, and data analytics"*, (2018).
[9]. Guthrie, J. J., *"CFD simulations on a Raspberry Pi cluster"*, Frankfurt am Main, (2015). DOI: 10.13140/RG.2.1.1079.2486
[10]. Michael A. Willcox, *"Solid rocket motor internal ballistics simulation using three-dimensional grain burnback"*, Propulsion and power, vol. 23, no 3, (2007). DOI: 10.2514/1.22971
[11]. Jiří Blazek, *"Computational Fluid Dynamics: Principles and Applications"*, Butterworth-Heinemann, (2015).

TÓM TẮT

Nghiên cứu tính toán thuật phóng trong động cơ tên lửa nhiên liệu rắn bằng phương pháp mô phỏng đa bước

Bài báo trình bày nghiên cứu tính toán thuật phóng trong động cơ tên lửa nhiên liệu rắn sử dụng phương pháp mô phỏng đa bước. Phương pháp này sử dụng công cụ CFX để mô phỏng quá trình nhiệt động của sản phẩm cháy trong buồng đốt và loa phụt theo thời gian. Sự thay đổi của mô hình tính toán được cập nhật sau mỗi bước thời gian, phản ánh chân thực quá trình thay đổi hình dạng liều nhiên liệu và sự mở rộng thể tích của buồng đốt. Nghiên cứu được áp dụng tính toán cho động cơ nhiên liệu rắn có đường kính trong 360mm, sử dụng liều nhiên liệu hình trụ một lỗ được tạo rãnh không hoàn toàn. Kết quả thử nghiệm thực tế đo lực đẩy động cơ cho thấy sai số dưới 2,5% so với mô phỏng, chứng minh tính chính xác của mô hình. Nghiên cứu góp phần cung cấp cơ sở khoa học cho việc phát triển các công cụ mô phỏng hiện đại, hỗ trợ thiết kế và dự đoán đặc tính làm việc của động cơ tên lửa trong điều kiện thực tế, giúp giảm chi phí thử nghiệm, đặc biệt đáng kể đối với động cơ có kích thước lớn, giá thành sản xuất cao.

Từ khóa: Động cơ nhiên liệu rắn; Thuật phóng trong; Mô phỏng đa bước; Nhiên liệu hỗn hợp; Bề mặt cháy phức tạp.